Original Study **Open Access**

Muhammad Irfan, Ali Murtaza Rasool*, Mubashir Aziz, Umair Ali, Fawad Niazi, Taro Uchimura

Development of Wetting-Drying Curves from Elastic Wave Velocities Using a Novel Triaxial Test Apparatus

https://doi.org/10.2478/sgem-2024-0006
received September 15, 2023; accepted March 11, 2024.

Abstract: The relationship between the soil water characteristic curve (SWCC) and the mechanical behavior of unsaturated soil is imperative and has been well investigated. However, the correlation between elastic wave velocity along the wetting and drying paths of SWCC is largely unknown due to the nonavailability of a standard experimental setup for such a purpose. An ordinary triaxial apparatus has been modified for laboratory assessment of SWCCs under different K_o stresses, along with the measurement of shear and compression wave velocities in due course. The main aim of the study is to draw SWCC, wave velocity characteristic curve (WVCC), and a Poisson's ratio characteristic curve (PRCC) and to establish the phenomenon that these curves possess hysteresis. The Poisson's ratio was obtained indirectly by measuring Vp and Vs. Three soil samples with relative densities of 85%, 56%, and 39% were prepared and placed in a modified triaxial test apparatus under wetting and drying cycles. The test results showed that the newly developed apparatus is accurately capable of measuring SWCC. Owing to the similarity in the shape of wave velocity and Poisson's ratio, response to SWCC, WVCC, and PRCC are drawn. The phenomenon of stress history and the effective stress of the soil affected the behavior during wetting and drying paths.

Keywords: Triaxial test; soil water characteristic curve; wave velocity characteristic curve; Poisson's ratio characteristic curve; elastic wave velocity.

1 Introduction

Industrialization in recent decades has led to an increase in global temperatures with significant effects on climatic conditions such as higher-intensity rainfalls and an increase in water vapor-carrying potential of air. From the geotechnical engineering perspective of seasonal moisture variations in unsaturated soils, climate change has contributed to more frequent slope failures causing severe damage to infrastructure and human life. Hence, it becomes crucial to characterize the hydraulic and mechanical behavior of unsaturated soils, which is largely influenced by stress state and drainage conditions [1–7]. According to Rahardjo et al. [8], a slope may fail during rainfall that could stand safely in a dry season because an additional shear strength is present just above the water table and within the boundaries of the unsaturated zone. Therefore, active monitoring of moisture variations in a slope is necessary to predict its failure [9]. Typical monitoring systems for the measurement of matric suction of soil include tensiometers or ceramic cups as well [10], and for measuring the volumetric water content of the soil, dielectric moisture sensors are used [11]. All these being point sensors, they are only sensitive to changes in the moisture content locally occurring in the proximity of the sensor. Such sensors would be required in large amounts possibly if a landslide area with a wide potential is to be covered. A novel idea to predict the variation in soil moisture is to monitor wave velocities. Irfan et al. [12] developed a modified triaxial apparatus for the determination of elastic wave velocities

***Corresponding author: Ali Murtaza Rasool,** National Engineering Services Pakistan (NESPAK), Lahore 54700, Pakistan, E-mail: ali_eng@hotmail.com, ali.murtaza@nespak.com.pk
Muhammad Irfan, Birudo Engineers, 90-A4 (Second Floor), Sharif Colony, Canal Park, Gulberg-II, Lahore 54700, Pakistan
Mubashir Aziz, Umair Ali, Department of Civil & Environmental Engineering, King Fahd University of Petroleum & Minerals, Dhahran 31261, Saudi Arabia; Interdisciplinary Research Center for Construction & Building Materials, King Fahd University of Petroleum & Minerals, Dhahran 31261, Saudi Arabia
Fawad Niazi, Department of Civil and Mechanical Engineering, Purdue University Fort Wayne, USA
Taro Uchimura, Graduate School of Science and Engineering, Saitama University, Saitama 338-8570, Japan

alongside performing infiltration tests on unsaturated soil samples, and Irfan et al. [13] further studied the effects of saturation and deformation of the soil on wave velocities in the context of predicting rainfall-induced landslides. Predicting temporal variations in the soil moisture by measurement of the wave velocities is done by using a receiver assembly and an elastic wave exciter combined on the surface of the slope. Through them, elastic wave velocities are monitored with the change in soil moisture. A combination of receiver and exciter system can be used to cover a wide area of slope in this way [14, 15].

Likewise, the physical properties of unsaturated soil take on the form of a nonlinear function of suction, which can vary from zero to a million kilopascals depending on the climatic conditions [16]. The behavior of an unsaturated soil sample is primarily influenced by its soil water characteristic curve (SWCC), which shows the correlation between the amount of water in the soil pores (measured in terms of volumetric or gravimetric water content, saturation ratio, etc.) and the soil matric suction [17–19]. For a better understanding of the behavior of unsaturated soils, various researchers [20–22] have explored the variation of soil parameters along the wetting/drying path of SWCC. Gallage et al. [23] studied the unsaturated hydraulic conductivity function in SWCC along the drying and wetting paths and concluded that the hydraulic conductivity of unsaturated soils depends on several factors, such as the quantity of water present inside the soil skeleton. Hence, irrespective of the wetting or drying path, hydraulic conductivity is the same when the same amount of water exists in the soil skeleton. Zhai et al. [24] introduced a framework that utilizes the pore size distribution function (PSDF) concept to estimate SWCCs for various initial void ratios. The authors validated their approach by comparing their results to experimental data reported in previous studies. Likos et al. [25] developed a relative humidity technique to measure total suction characteristic curves, which was implemented recently by Patil et al. [26] who combined the axis translation technique with the relative humidity technique to obtain SWCC of soil samples over a wide range of suction between 0.05 and 300 MPa.

Determination of SWCC requires the availability of specialized laboratory equipment and is usually performed in a pressure plate apparatus [27] or a Tempe pressure cell [28]. However, no standard apparatus is available for the determination of elastic wave velocities during the wetting and drying paths of SWCC, with limited research on correlating elastic wave velocities with the soil water retention curve [29, 30]. Kassab et al. [31] performed an experimental study to describe the behavior of both primary wave (P-wave) and secondary wave (S-wave) velocities using sandstone samples that are porous, irrespective of whether the conditions are dry or wet. They observed that the obtained linear equations can be used to estimate S-wave from P-wave velocity, no matter what the condition is, that is, wet or dry sample state. Taylor et al. [32] designed a near-surface soil water retention curve (SWRC) laboratory device in which unconfined specimens in a controlled temperature chamber were subjected to three-dimensional vapor flow. The preliminary results provided insight into the discrepancies between unconfined and confined unsaturated soil behavior. Nevertheless, the behavior of elastic waves during the wetting path of SWCC is still largely unexplored. Another important elastic property of the soil is Poisson's ratio, which is the ratio of lateral strain to longitudinal strain under uniaxial loading [33]. SWCC is required as an input for numerous analytical analyses and numerical simulations, spanning from slope stability, earth pressure, settlement, and bearing capacity to swelling and shrinkage [25, 34]. Experimental determination of a soil's Poisson's ratio can be carried out by measuring its shear and compressional wave velocities using methods such as the bender element method, ultrasonic testing devices, and piezoelectric transducers [35–37]. Thota et al. [38] presented a concept of Poisson's ratio characteristic curve (PRCC), which established a relationship between Poisson's ratio and the degree of saturation (or matric suction). Similar to SWCC, no researcher has been able to predict Poisson's ratio behavior along the wetting and drying paths. Therefore, in this study, development of wetting drying curves from elastic wave velocities using novel triaxial test apparatus has been done. For this purpose, a novel triaxial apparatus was designed to not only determine the SWCC varying magnitudes of K_o stress, but also to be able to measure shear and compression wave velocities in due course. The primary objective of this research is to draw SWCC, wave velocity characteristic curve (WVCC), and PRCC along its wetting and drying paths in unsaturated soils. The Poisson's ratio was obtained indirectly by measuring Vp and Vs. Recognizing the gap in existing knowledge and the lack of standard experimental setups to investigate this correlation, the authors have modified a conventional triaxial apparatus. This modification enables us to comprehensively assess various characteristic curves under varied Ko stresses while concurrently measuring both shear and compression wave velocities. Through this innovative approach, our study aims to provide new insights into the mechanical behavior of unsaturated soils, a critical aspect in the field of geotechnical engineering.

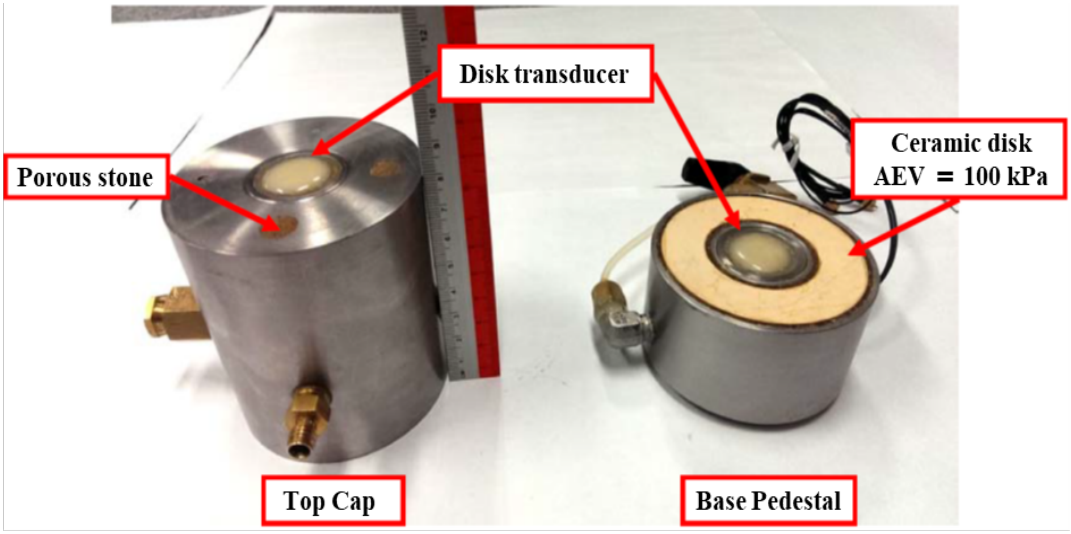

Figure 1: Modified pedestal and top cap of triaxial apparatus, fitted with disk-type piezoelectric transducers at their respective centers.

2 Equipment Design

The addition of an elastic wave measurement system to a triaxial apparatus has been modified to enable the measurement of SWCC under constant total stress conditions. The configuration of the apparatus is shown in Figure 1. The base pedestal of the apparatus contains a ceramic disk ① that is shaped like a donut embedded in it. The ceramic disk used has air entry value (AEV) = 100 kPa and, as such, the apparatus is limited to testing of the sands only. There is also a piezoelectric disk transducer ② right in the middle. For the preparation of specimens (with a diameter of 75 mm and height of 41 mm), a latex membrane ③ was used that was supported by a brass split mold ④. During the whole experiment, the split mold was kept in place to avoid the risk of expansion or contraction in the sample. During the test, the top cap was allowed to move freely in case of any vertical movement. The specimens were subjected to effective K_o stress conditions. As the top cap was allowed to move freely, its movement was recorded using a vertical rod with attached LVDT ⑤ connected to the top cap. By modifying the dead loads ⑥ placed at the top of platform ⑦ directly attached to the top cap, any variations in vertical stress were negated effectively. It is explicitly stated that while a triaxial apparatus was used, the tests were performed under oedometric conditions with specific modifications to suit our study requirements.

Deaired water was used for saturating the specimen. By keeping an eye on water entering inside or coming out of the specimen, the saturation state of the specimen was kept in check. For measurement of water entering inside or getting out, a water bottle ⑧ was attached to the ceramic disk, and its weight was monitored all the time. In that bottle, the pressure of water was atmospheric ⑨. This was achieved by drilling a hole in the upper portion of the bottle. Another similar water bottle setup was established to measure the evaporation losses through this manually drilled hole. Evaporation losses were later used to adjust the weight of the bottle attached to the specimen sample. The water bottle was constantly monitored to keep track of anything entering inside or going outside. This was achieved by placing the bottle over a weighing balance ⑩ while constantly picturing the readings at the designated time interval.

3 Test Procedure

3.1 Physical Properties of the Soil

In this study, Edosaki sand sourced from a natural slope in Ibaraki, Japan, was utilized. For all the experiments, the gravimetric water content percentage was set at 10%. The sand has specific gravity Gs = 2.71, maximum dry density, $g_{d\max}$ = 1.762 g/ml, minimum void ratio, $e_{\min}$ = 0.647, and maximum void ratio, $e_{\max}$ = 1.16. The initial height of the specimen was 40 mm, whereas the diameter was 74 mm. Three specimens having relative density (Dr) of 85%, 56%, and 39% were prepared and tested.

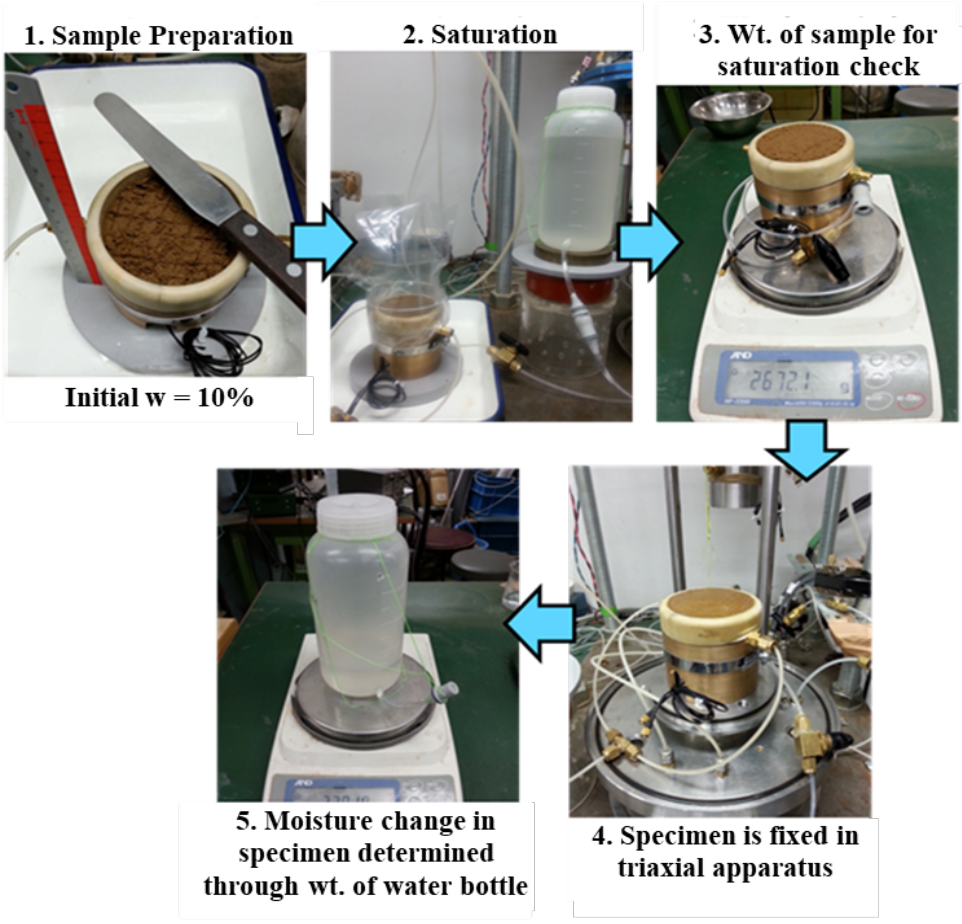

Figure 2: Specimen preparation and saturation.

3.2 Specimen Preparation and Saturation

In the experiment, there were a variety of procedures involved. The procedures involve saturating the ceramic disk, sample preparation, and acquiring SWCC for drying and wetting with elastic wave measurements. The first step of the test was to saturate the ceramic disk. For this purpose, it was dipped inside a water container. The negative pressure ceramic disk was subjected to was –101.78 kPa. It was immersed inside the tank for 24 h. After that, it was taken out and fitted in the triaxial apparatus. To negate the risk of desaturation, a water bottle was attached to it. As the next step for setting up of split mold, a 0.3-mm-thick rubber membrane was added on the circumference of the base pedestal. Computation of the weight of the overdried Edosaki sand in question was done for achieving the required density. Edosaki sand sourced from a natural slope in Ibaraki, Japan, was utilized. For all the experiments, the gravimetric water content percentage was set at 10%. Water was added to the soil sample and mixed thoroughly to achieve this target. As the ceramic disk was saturated, any connection of water to the disk was stopped right there and the surface was dried with the help of tissue paper. For preparation of the sample, a wet tamping technique was used. In this technique, the wet soil was tamped into four identical layers. The sample preparation was done on top of the ceramic disk. Saturation of the sample was achieved by water flow through the ceramic disk. However, the water head was kept quite minimal (1–2 kPa) to negate any chances of piping occurring inside the sample. Together, all the apparatus (the base pedestal and the mold, excluding the water bottle) alongside the soil sample was weighed at specified intervals. Attainment of constant weight indicated saturation of the sample. It took 3–4 days to achieve the saturation point. Figure 2 shows all the steps involved in the preparation and saturation of the specimen.

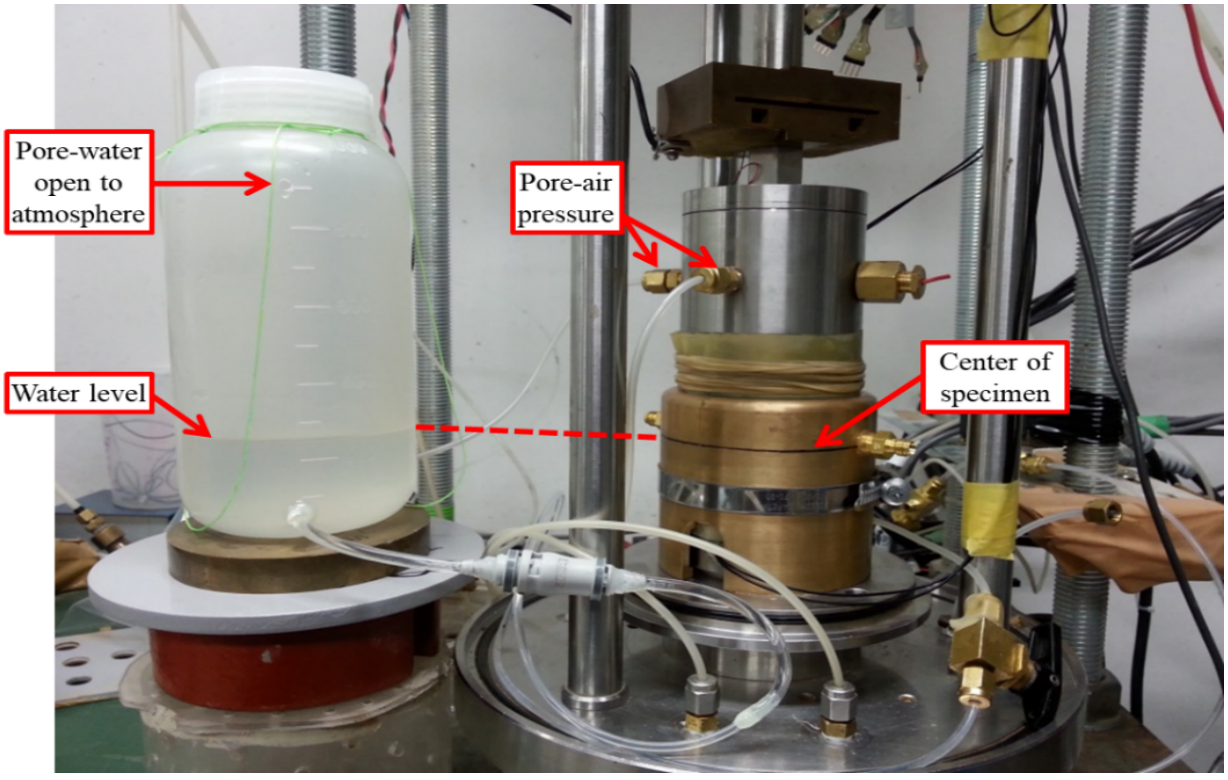

Figure 3: Water injection/drainage setup.

3.3 Determination of Drying and Wetting SWCC

Once the soil specimen was prepared, it was subjected to matric suction of various distinctive magnitudes. The changes in moisture of the sample were recorded and used for the determination of wetting and drying SWCC. After the setup was achieved, the center of the specimen was marked and the water in the bottle was brought to exactly that point. Pore air pressure present inside the specimen was reduced to zero, that is, $u_{a=}0$ (Figure 3). This was an indication of zero matric suction ($u_a - u_w = 0$). This condition was sustained until the achievement of a constant water bottle weight. After this, the drying path started. During the drying process, the matric suction was incrementally increased to 0.5, 1.0, 2.0, 4.0, 7.0, 10.0, 15.0, 30.0, and 50.0 kPa, respectively. Lower values of matric suction, that is, between 0 and 4 kPa, were achieved by lowering the water level in the bottle. During this, the pore air pressure was kept at 0. Numerically, for the application of 4 kPa suction pressure, a 40-cm lowering of the water level was done. Beyond 4 kPa, the water level was returned to the original position and was not disturbed. Using the top cap, the pore air pressure was enhanced for suction greater than 4 kPa. During the experiment, the applied pore air pressure was equal to the magnitude of the applied suction. To maintain a constant axial stress throughout the experiment, a counterweight equivalent to the magnitude of the applied pore air pressure was placed on the top cap.

Every increment in the matric suction resulted in water flowing outside the specimen. This kept on going until an equilibrium position was attained. The time taken to reach the equilibrium condition was around 24–48 h. It was indicated when the weight of the water bottle became constant. Shear and compression wave velocities were determined after the attainment of equilibrium. The water bottle and the soil specimen were linked by a non-spill coupling valve that was disconnected for measurement of water drained out of the specimen. The water bottle was weighed for this purpose after disconnection. The other bottle in the apparatus for measuring water losses due to evaporation was also weighed to apply the required corrections. The entry value of the air into the ceramic disk is the limiting factor for the maximum suction pressure. For this apparatus, the maximum pressure that can be applied was 100 kPa. However, in the present study, the application of suction beyond 50 kPa was practically impossible because, beyond this limit, the airtightness of the system was remarkably difficult to maintain. For simulation of the wetting path, the value of pore air

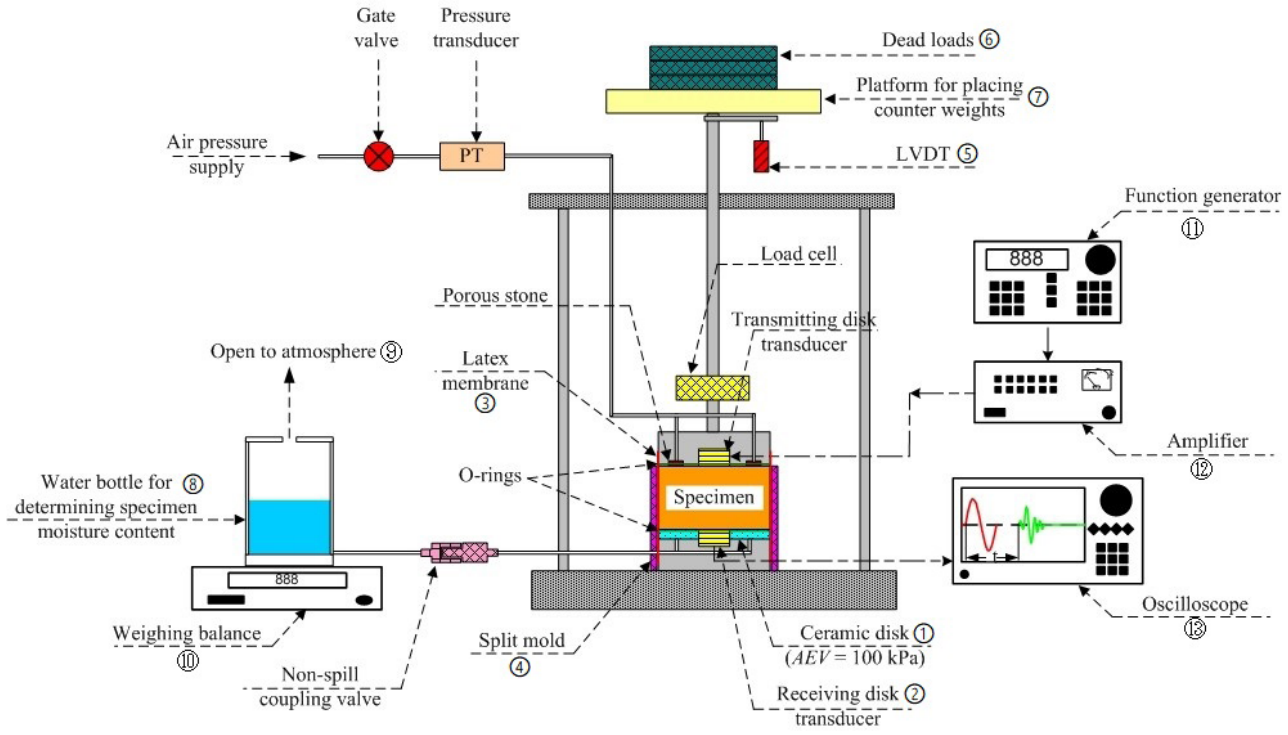

Figure 4: Schematic layout of modified SWCC wave velocity apparatus.

pressure was lowered from this value, that is, from 50 kPa. This was done alongside maintaining the water level at the required position, that is, at the center of the sample. As soon as the pore air pressure decreased, water started flowing into the specimen. This flow occurred through the ceramic disk. This kept on going until equilibrium was established. Again, the water bottle was disconnected from the apparatus. The weight of the bottle was determined to figure out the amount of water that flowed inside the specimen. For matric suction values higher than 4 kPa, the procedure remained the same. However, below 4 kPa values, the procedure used was different. The values were applied by venting the pore air pressure to the atmosphere, and then lowering of the water level was done below the center point position.

3.4 Elastic Wave Velocities

The shear and compression wave velocities were determined after the attainment of equilibrium using disk-type piezoelectric transducers [39, 40]. The apparatus used in this study has components of wave-measuring setup. The equipment used in the experiment included a Tektronix AFG3022B function generator (marked as ⑪), an NF Corp. HSA4012 power amplifier (marked as ⑫), and a HIOKI 8860 digital oscilloscope with a HIOKI 8957 high-resolution input module (marked as ⑬). A schematic diagram of the apparatus is shown in Figure 4 for a better understanding.

3.4.1 Determination of Elastic Wave Velocities

The calculation of wave velocities can be based on the basic formula for velocity, which relates the distance traveled to the time elapsed. By using specific formulas, it was possible to determine the compression wave *(Vp)* and shear wave *(Vs)* velocities in this study.

$$V_p = H/t \quad (1)$$

$$V_s = H/t \quad (2)$$

The distance traveled by a wave (H) can be determined based on the time it takes for the wave to travel that distance. In this study, the time of flight for compression and shear waves was used to calculate the corresponding travel distances.

The travel time, denoted as t, of each wave was determined by examining the response of both the transmitted and received signals. In the case of compression waves, the initial deflection in the receiver signal was identified as the arrival time of the compression

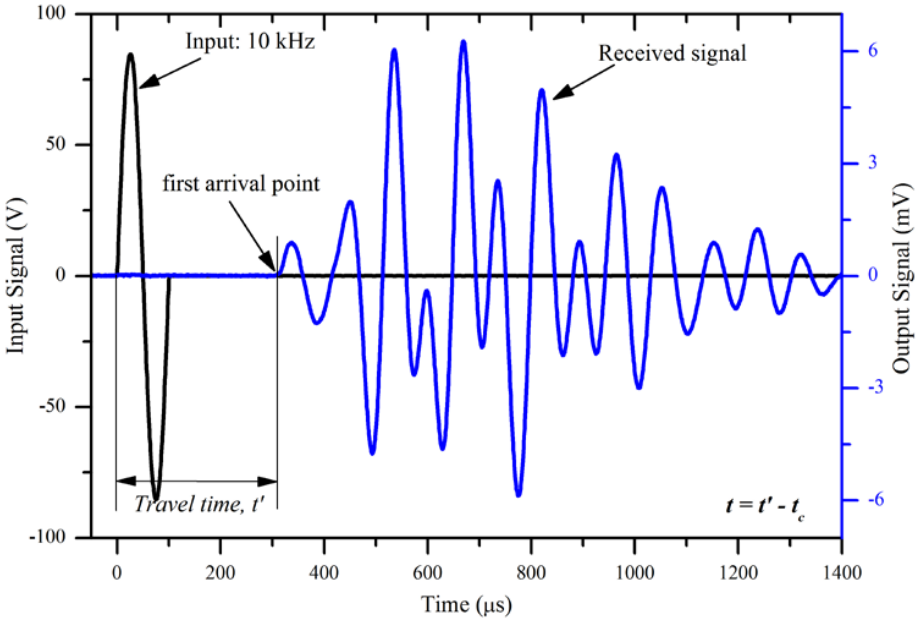

Figure 5: Travel time determination of compression wave signals.

wave. This interpretation of the first arrival time is appropriate because compression waves propagate the fastest and therefore arrive at the receiver before any other wave. Thus, the time between the first deflection of the input and output signals was used to calculate the flight time of the compression waves, as depicted in Figure 5.

Determining the travel time of shear waves is more complex than that of compression waves. This is because the initial deflection in the shear wave signal may not correspond to the arrival of the S-wave itself, but instead to the arrival of the "near-field" component, which propagates at the velocity of P-waves [41]. To calculate the travel time of the shear wave while ignoring the initial disturbance caused by the P-wave and the near-field effect, the "first-zero cross over" method was utilized [29]. Specifically, the travel time of the shear wave was estimated as the difference between the start of the transmitted signal and the start of the first significant positive polarity increase, as depicted in Figure 6.

To measure the velocity of elastic waves, an excitation voltage was generated by a function generator and amplified by a power amplifier. This voltage was then applied to the transmitter disk transducer. The wave propagated through the soil specimen and was received by the receiver disk transducer located at the top cap. The received signal was then transferred to a digital oscilloscope for display. The input signal from the power amplifier was also sent to the oscilloscope via a monitoring channel, allowing for simultaneous recording of both the input and output signals. The process of determining elastic wave velocities (*Vs* and *Vp*) was conducted in a similar manner to that of the drying path, which involved equalizing matric suction at each level. The whole assembly was disconnected when zero matric suction was achieved during the wetting process. After that, the specimen was oven-dried and moisture content was determined through it. This moisture content and water bottle readings determined at different suction levels were used to calculate the corresponding moisture content of the specimen. This moisture content was obtained at various suction levels.

4 Results and Discussion

4.1 Soil water characteristic curve

A series of tests have been conducted on the Edosaki sand with 85% relative density under the effect of net normal stress (σ-u_a) 10 kPa. Contrary to a typical SWCC test, a small net stress was required in this case to establish sound contact between the disk transducer and soil. Without the establishment of this contact, the transmission of elastic waves from the sensor to the soil was not possible. *SWCC* of the studied soil is presented in Figure 7, and the correlation of *SWCC* is carried out with the established [42] model. Fitting data confirm that the results of *SWCC* are reliable and consistent with the results of [23].

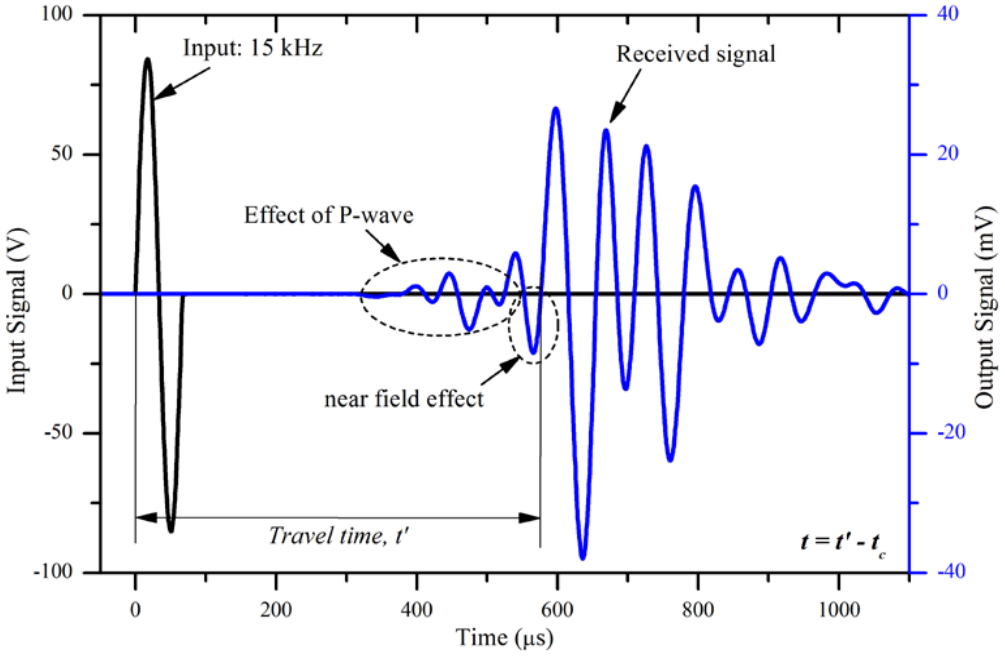

Figure 6: Travel time determination of shear wave signals.

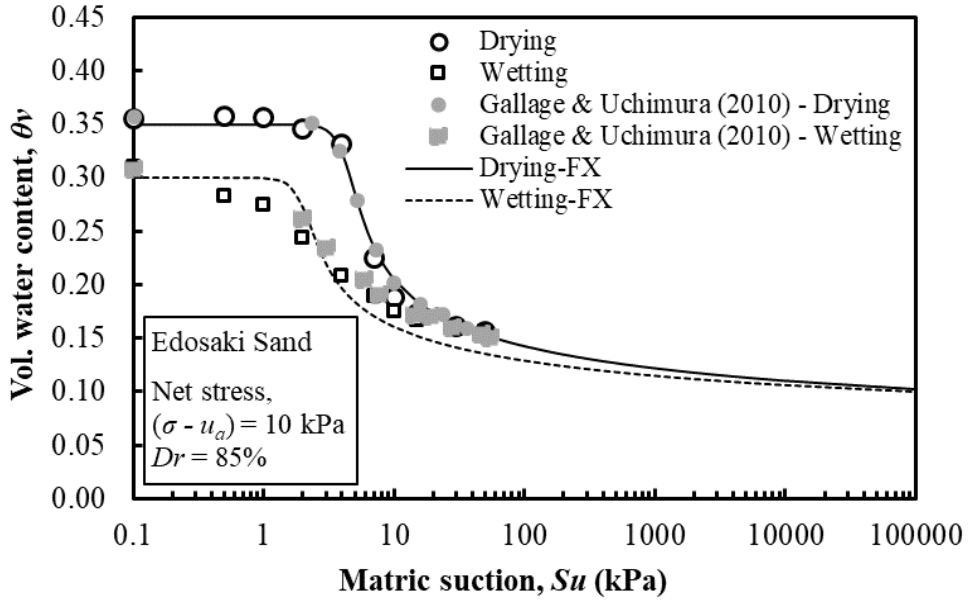

Figure 7: Soil water characteristic curve (SWCC) of Edosaki sand.

4.2 Initial test results along with the repeatability

A test series (Series-01) was performed on the specimen prepared at 85% relative density and under the effect of net normal stress (σ-u_a) 10 kPa. Figure 8a, b shows that the shear and compression wave velocities increase with the matric suction. The graph shows that the indicated behavior is bilinear with a depiction of clear hysteresis that is between the wetting and the drying curves. An increase in matric suction is accompanied by a decrease in water content of the soil. Dry soils are relatively stiff and may have contributed to the increase in wave velocities. The graphs show that both shear and compression wave

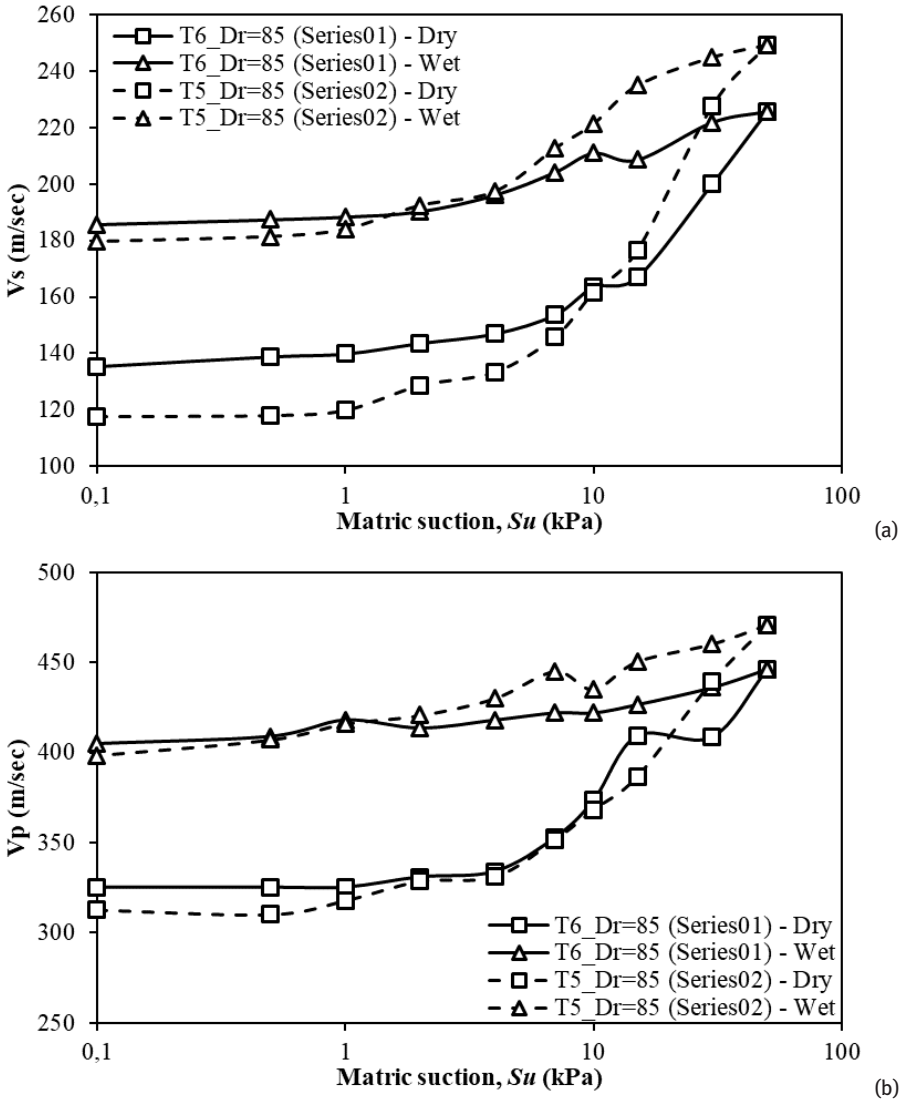

Figure 8: Relationship b/w suction and (a) shear wave velocity, (b) compression wave velocity.

velocities increase with matric suction. Effective stress between soil particles is enhanced by suction, thereby facilitating the propagation of waves through the soil skeleton. A direct relationship is, therefore, observed between matric suction and wave velocities. This is further substantiated by the fact that an increase in suction is accompanied by a decrease in the water content of the soil (as shown in Figure 7). Dry soils are relatively stiff and possess high modulus, that is, high wave speed [43]. The reliability and accuracy of the measurements was verified by performing another test series (Series-02) at 85% relative density and effect of net normal stress (σ-u_a) 10 kPa. The test results of the second series performed to determine the reliability and accuracy are shown in Figure 8 (a, b). A comparison of graphs demonstrates the direct dependence of wave velocities on the matric suction of soil. Wave velocities increase/decrease nonlinearly with an increase/decrease in matric suction. It can be noted that the results of tests performed in Series-01 and Series-02 as shown in the figure are comparable. This justifies the reliability and repeatability of experimental work.

4.3 Relation between matric suction, compression, and shear wave velocities and volumetric water content

Figure 9 shows the effect of variation of relative densities on matric suction, compression, and shear wave velocities with volumetric water content. For each specimen

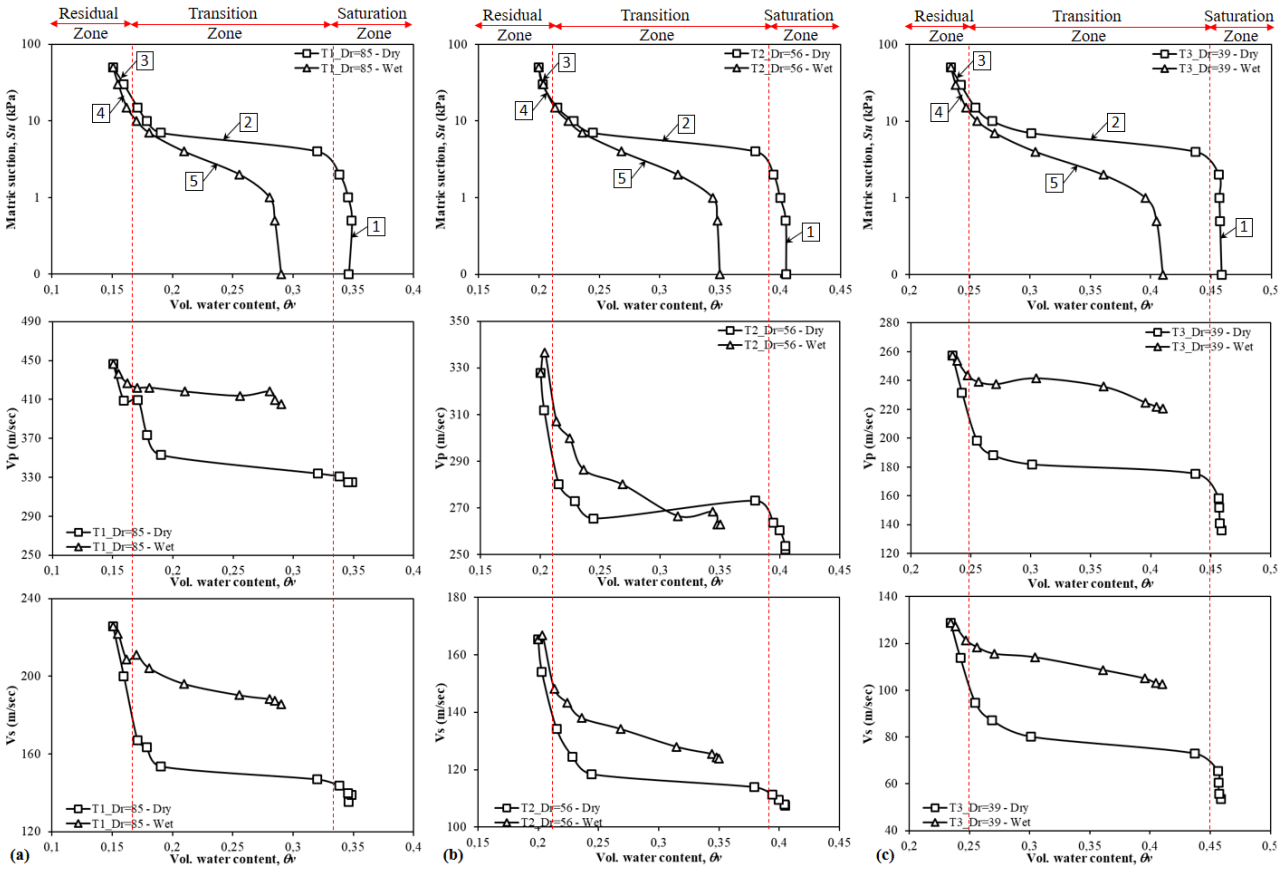

Figure 9: Effect of variation in relative density on matric suction, shear wave velocity, and compression wave velocities with volumetric water content.

variation, matric suction, compression wave velocity, and shear wave velocity have been drawn, which show a bilinear behavior that depicts a clear hysteresis between the drying and wetting curves. Various researchers [12, 13, 29, 44] have shown the dependency of wave velocities on soil moisture. The general trend observed in the figure is similar as wave velocities increase with decreasing soil moisture and vice versa. Owing to the similarity in shape of wave velocity response to SWCC, the curve is being termed as WVCC. Identical to SWCC, WVCC of each specimen shows three distinct zones: saturation zone, transition zone, and residual zone. In the saturation zone, during the drying path, water is pushed out of the soil. At the start of the experiment, upon an increase in matric suction, air starts entering the soil skeleton, but is yet to break the surface tension of water. Before reaching AEV, water does not get pushed out of the soil skeleton, but effective stress increases due to an increase in matric suction. Thus, an increase in matric suction in this saturation zone leads to an increase in effective stress between soil particles. An increase in particle-to-particle contact stress causes an increase in wave velocities. In the transition zone, water is ejected from the soil rapidly without any significant change in matric suction. An increase in wave velocity follows a similar trend to matric suction (i.e., no rapid rise). In the residual zone (drying), wave velocities increase rapidly since effective stress increases due to matric suction. An increase in wave velocity is further substantiated by the ejection of water from the specimen, that is, the drier the specimen, the higher will be its modulus/wave velocity. In the residual zone (wetting), a decrease in matric suction causes a loss of effective stress. As the particle-to-particle contact force diminishes, wave velocities start decreasing. The pattern of compression wave velocities in unsaturated specimens exhibits similarities with that of shear wave velocities, but with a magnitude nearly twice as large. It is interesting to note that the wave velocities for the same matric suction during the wetting and drying parts is different, thereby causing a hysteresis identical to SWCC. A possible explanation for this phenomenon can be attributed to the stress history of soil. When a virgin soil sample is dried by an increase

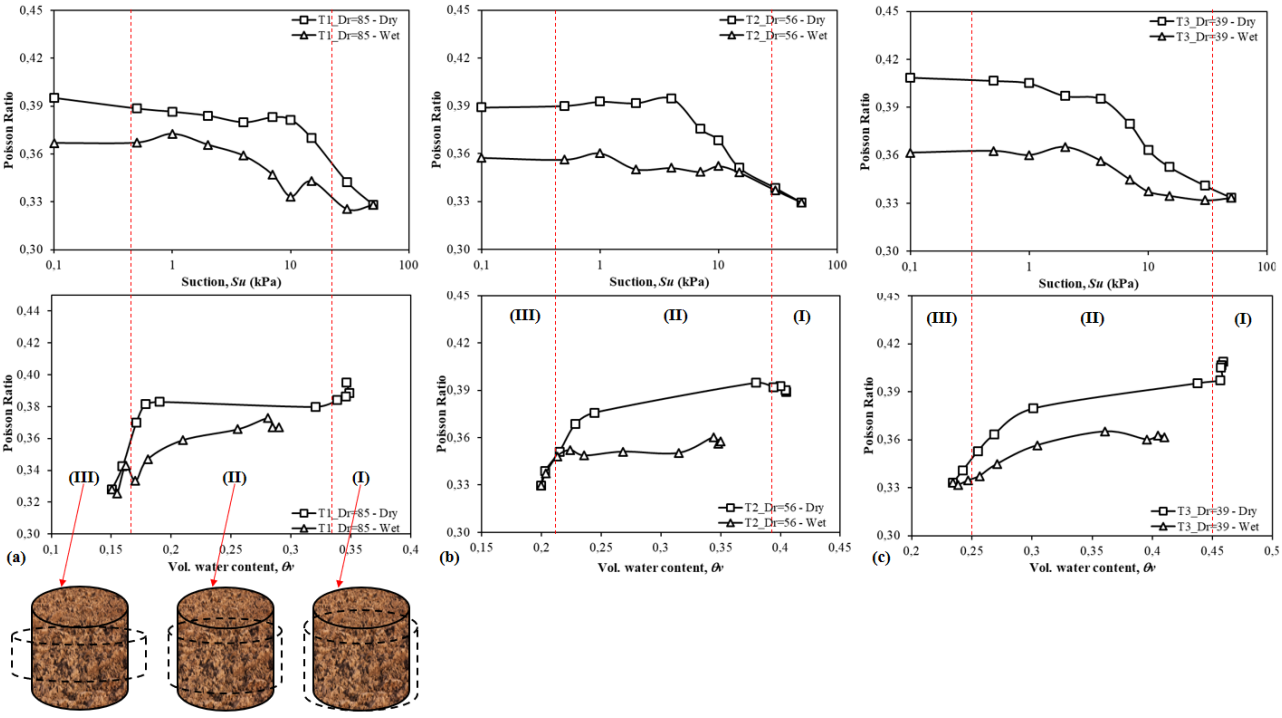

Figure 10: Measured Poisson's ratio versus matric suction and volumetric water content.

of matric suction, the soil "remembers" the stress history and even upon release of applied matric suction, the effective stress between soil particles is not completely lost. A stronger particle-to-particle contact during the wetting phase, therefore, causes higher wave velocities. This phenomenon may, however, be related to the stress path the sample has been subjected to during these tests, that is, drying of an initially wet sample and subsequent wetting. A comparison of graphs also demonstrates direct dependence of wave velocities on the matric suction of soil. Wave velocities increase/decrease nonlinearly with an increase/decrease in applied matric suction.

4.4 Relation between Poisson's ratio versus suction and volumetric water content

Poisson's ratio, which is defined as the ratio of the lateral strain to the longitudinal strain under uniaxial loading, is an elastic property of soil. Instead of directly measuring lateral and longitudinal strains, the authors inferred Poisson's ratio indirectly through the measurements of shear and compression wave velocities in the soil specimens. Figure 10 depicts the experimental determination of Poisson's ratio based on the measurements of shear and compression wave velocities [33, 45]. The figure includes a *PRCC* [38], which, similar to SWCC and WVCC, relates the Poisson's ratio to the degree of saturation and matric suction. PRCC follows three distinct water retention regimes and exhibits variations between the dry and saturated states. At the dry state (I), the Poisson's ratio is minimal due to the high compressibility of the soil. Conversely, at the saturated state (III), the soil becomes almost incompressible, resulting in a maximum Poisson's ratio. Hence, there exists an inverse relationship between Poisson's ratio and soil compressibility. As the soil undergoes a transition from saturated to unsaturated state, both the degree of saturation and Poisson's ratio decrease at varying rates, depending on the dominant water retention state. Laboratory measurements reveal that the rate of change in the Poisson's ratio is higher when the water content decreases, resulting in increased soil compressibility [38, 39]. In the saturated state (capillary state), the Poisson's ratio undergoes minimal changes. This is because the compressibility of water is negligible compared to that of the soil matrix. Therefore, in the near-saturated condition, the pore water dominates over the soil skeleton, leading to a high and relatively constant Poisson's ratio. The Poisson's ratio value in the saturated state represents stage III in PRCC. Due to the stress history of soil, the drying and wetting curves show some difference in Poisson's ratio values. However, for different relative densities, there is very little difference in final values.

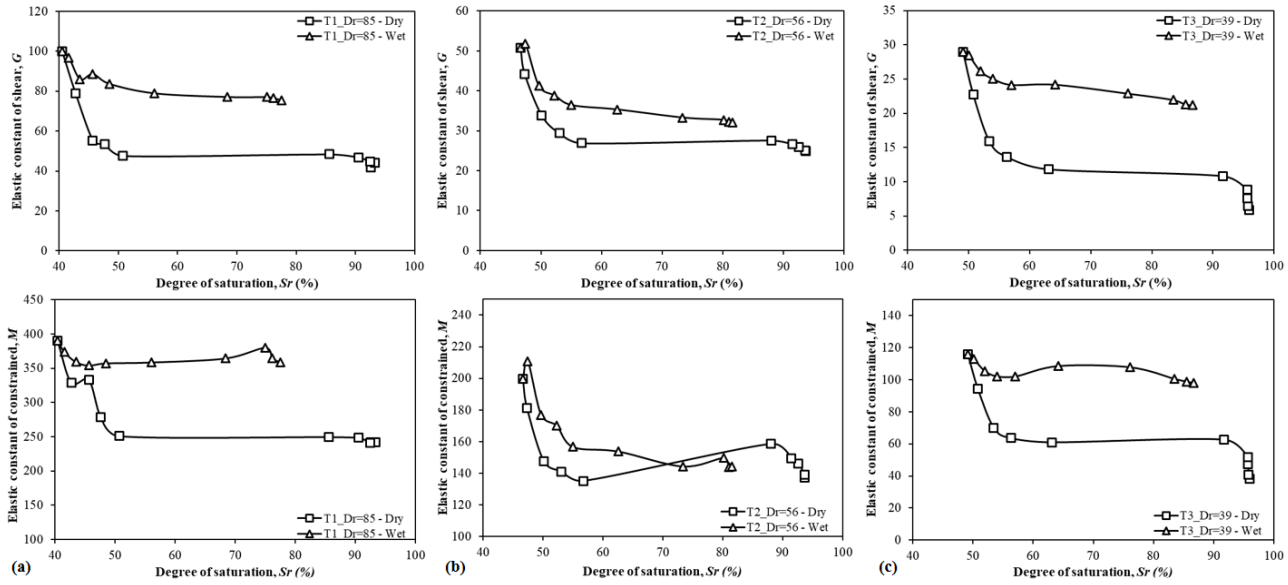

Figure 11: Relation between soil moduli and degree of saturation.

4.5 Relation between soil moduli and degree of saturation

Elastic moduli such as Young's modulus and shear modulus are measures of the stiffness of materials that respond to recoverable deformations. For materials that are elastic, isotropic, and homogeneous, the elastic constants are given by the following equations [46].

$$G=\rho V_s^2 \tag{3}$$

$$M=\rho V_p^2 \tag{4}$$

The elastic constants of shear and constrained, denoted as G and M respectively, are important parameters for evaluating the immediate settlement and dynamic response of geotechnical structures in engineering practice. These constants can be determined based on shear and compressive wave velocities, denoted as Vs and Vp, respectively, for materials that are elastic, isotropic, and homogeneous. Figure 11 illustrates the variations in G and M for different relative densities under different degrees of saturation. It can be observed that the elastic constants of shear and constrained tend to increase as the degree of saturation decreases due to drying. The moduli exhibit gradual increases during the early stages of drying, with more significant changes observed as the drying progresses. The observation in this point is, however, interesting from a practical viewpoint, wherein the modulus of soils in the vadose zone can be expected to show similar hysteresis, for example, a soil layer having seasonal fluctuations of water (i.e., lowering followed by an increase in water level) is expected to demonstrate a higher modulus (i.e., lower settlement potential) the following year. The graphs show a clear hysteresis for both wetting and drying curves and a difference in both curves due to the possible stress history of the soil. The values for the elastic constant of constrained are approximately four times the values of the elastic constant of shear. The specimens with higher relative density showed more values of both elastic constants.

5 Summary

The authors have developed a novel apparatus to investigate the changes in shear and compression wave velocities as the Edosaki sand undergoes drying and wetting along SWCC. To the best of their knowledge, there is currently no standardized apparatus available for this purpose. In this article, the authors explain the underlying principles of their apparatus and discuss its practical limitations. The authors also assess the effectiveness of their apparatus by comparing the preliminary test results with previously published data. The following main conclusions are derived from the presented work:

– A direct relationship between the shear wave velocities and the matric suction was observed. The increased effective stress and stiffness due to increasing matric suction resulted in increased wave velocities.

- WVCC showed a similar trend to SWCCs with a change in suction and density of the soil. Like SWCC, WVCC also showed a hysteresis behavior, which can be attributed to the stress history of the soil. Furthermore, the wetting/drying paths possessed different matric suction values, which affected the wave velocities as well. A nonlinear relationship was observed between the wave velocity and the applied matric suction.
- PRCC showed a similar trend of hysteresis during wetting and drying paths. The Poisson's ratio was observed to be maximum at the saturated stage due to the incompressible nature of the soil of the sample and was minimum at the dry stage.
- The elastic constants of shear showed a direct relation with the sample saturation level and matric suction with the hysteresis effect. The elastic constant of constrained was found to be approximately four times higher than the elastic constant of shear.

Data Availability Statement

The authors confirm that the data supporting the findings of this study are available within the article.

Acknowledgments

Department of Civil Engineering at The University of Tokyo, Japan, is gratefully acknowledged for the laboratory testing facilities.

Competing Interests

The authors have no relevant financial or non-financial interests to disclose.

References

[1] Macari EJ, Hoyos LR. Mechanical Behavior of an Unsaturated Soil under Multi-Axial Stress States. Geotechnical Testing Journal (2001). https://doi.org/10.1520/GTJ11278J

[2] Rasool AM, Kuwano J, Tachibana S. Experimental Study on the Response of Unsaturated Silt Due to Change in Drainage Conditions During the Triaxial Test Process. Geotechnical and Geological Engineering (2020). https://doi.org/10.1007/s10706-019-01125-3

[3] Rasool AM, Kuwano J. Effect of constant loading on unsaturated soil under water infiltration conditions. Geomechanics and Engineering (2020). https://doi.org/10.12989/gae.2020.20.3.221.

[4] Rasool AM, Aziz M. Advanced Triaxial Tests on Partially Saturated Soils Under Unconfined Conditions. International Journal of Civil Engineering (2020). https://doi.org/10.1007/s40999-020-00530-7

[5] Rahardjo H, Kim Y, Satyanaga A. Role of unsaturated soil mechanics in geotechnical engineering. International Journal of Geo-Engineering (2019). https://doi.org/10.1186/s40703-019-0104-8

[6] Wu D, Liu H, Wang C, Xu X, Liu X, Wang Q. The Interaction Effect of Particle Composition and Matric Suction on the Shear Strength Parameters of Unsaturated Granite Residual Soil. Arab J Sci Eng (2022). https://doi.org/10.1007/s13369-021-06503-9

[7] Al-Omari RR, Fattah MY, Kallawi AM. Laboratory Study on Load Carrying Capacity of Pile Group in Unsaturated Clay. Arab J Sci Eng (2019). https://doi.org/10.1007/s13369-018-3483-9

[8] Rahardjo H, Satyanaga A, Leong EC, Ng YS. Effects of groundwater table position and soil properties on stability of slope during rainfall. Journal of Geotechnical and Geoenvironmental Engineering (2010). https://doi.org/10.1061/(ASCE)GT.1943-5606.0000385

[9] Uchimura T, Towhata I, Wang L, Nishie S, Yamaguchi H, Seko I, et al. Precaution and early warning of surface failure of slopes using tilt sensors. Soils and Foundations (2015). https://doi.org/10.1016/j.sandf.2015.09.010

[10] Bittelli M. Measuring soil water potential for water management in agriculture: A review. Sustainability (2010). https://doi.org/10.3390/su2051226

[11] Xu J, Logsdon S, Ma X, Horton R, Han W, Zhao Y. Measurement of Soil Water Content with Dielectric Dispersion Frequency. Soil Science Society of America Journal (2014). https://doi.org/10.2136/sssaj2013.10.0429

[12] Irfan M, Uchimura T. Modified triaxial apparatus for determination of elastic wave velocities during infiltration tests on unsaturated soils. KSCE Journal of Civil Engineering (2016). https://doi.org/10.1007/s12205-015-0404-2

[13] Irfan M, Uchimura T, Chen Y. Effects of soil deformation and saturation on elastic wave velocities in relation to prediction of rain-induced landslides. Engineering Geology (2017). https://doi.org/10.1016/j.enggeo.2017.09.024

[14] Chen Y, Irfan M, Uchimura T, Meng Q, Dou J. Relationship between water content, shear deformation, and elastic wave velocity through unsaturated soil slope. Bulletin of Engineering Geology and the Environment (2020). https://doi.org/10.1007/s10064-020-01841-8

[15] Chen Y, Irfan M, Uchimura T, Cheng G, Nie W. Elastic wave velocity monitoring as an emerging technique for rainfall-induced landslide prediction. Landslides (2018). https://doi.org/10.1007/s10346-017-0943-3

[16] Fredlund DG, Fredlund MD. Application of 'estimation procedures' in unsaturated soil mechanics. Geosciences (Switzerland) (2020). https://doi.org/10.3390/geosciences10090364

[17] Puppala AJ, Punthutaecha K, Vanapalli SK. Soil-Water Characteristic Curves of Stabilized Expansive Soils. Journal of Geotechnical and Geoenvironmental Engineering (2006). https://doi.org/10.1061/(ASCE)1090-0241(2006)132:6(736)

[18] Rasool AM, Kuwano J. Influence of matric suction on instability of unsaturated silty soil in unconfined conditions. International Journal of GEOMATE (2018). https://doi.org/10.21660/2018.42.7115
[19] Matlan SJ, Taha MR, Mukhlisin M. Assessment of Model Consistency for Determination of Soil–Water Characteristic Curves. Arab J Sci Eng (2016). https://doi.org/10.1007/s13369-015-1888-2
[20] Yang H, Rahardjo H, Leong EC, Fredlund DG. Factors affecting drying and wetting soil-water characteristic curves of sandy soils. Canadian Geotechnical Journal (2004). https://doi.org/10.1139/t04-042
[21] Pasha AY, Khoshghalb A, Khalili N. A void ratio dependent water retention curve model including hydraulic hysteresis. E3S Web of Conferences (2016). https://doi.org/10.1051/e3sconf/20160911010
[22] Zapata CE, Houston WN, Houston SL, Walsh KD. Soil-Water Characteristic Curve Variability. Advances in Unsaturated Geotechnics (2020). https://doi.org/10.1061/40510(287)7
[23] Gallage CPK, Uchimura T. Effects of dry density and grain size distribution on soil-water characteristic curves of sandy soils. Soils and Foundations (2010). https://doi.org/10.3208/sandf.50.161
[24] Zhai Q, Rahardjo H, Satyanaga A, Dai G, Zhuang Y. Framework to estimate the soil-water characteristic curve for soils with different void ratios. Bulletin of Engineering Geology and the Environment (2020). https://doi.org/10.1007/s10064-020-01825-8
[25] Likos WJ, Lu N. Automated Humidity System for Measuring Total Suction Characteristics of Clay. Geotechnical Testing Journal (2003). https://doi.org/10.1520/GTJ11321J
[26] Patil UD, Hoyos L, Puppala A. Characterization of Compacted Silty Sand Using a Double-Walled Triaxial Cell with Fully Automated Relative-Humidity Control. Geotechnical Testing Journal (2016). https://doi.org/10.1520/GTJ20150156
[27] Perez-Garcia N, Houston S, Houston W, Padilla J. An Oedometer-Type Pressure Plate SWCC Apparatus. Geotechnical Testing Journal (2008). https://doi.org/10.1520/GTJ100964
[28] Rahardjo H, Nong XF, Lee DT, Leong EC, Fong YK. Expedited Soil–Water Characteristic Curve Tests Using Combined Centrifuge and Chilled Mirror Techniques. Geotechnical Testing Journal (2017). https://doi.org/10.1520/GTJ20160275
[29] Lee JS, Santamarina JC. Bender Elements: Performance and Signal Interpretation. Journal of Geotechnical and Geoenvironmental Engineering (2005). https://doi.org/10.1061/(ASCE)1090-0241(2005)131:9(1063)
[30] Deng JH, Dai JY, Lee JW, Lo WC. An Experimental Study on the Impact of Different-frequency Elastic Waves on Water Retention Curve. American Geophysical Union, Fall Meeting 2017, Abstract #H11G-1293 (2017)
[31] Kassab MA, Weller A. Study on P-wave and S-wave velocity in dry and wet sandstones of Tushka region, Egypt. Egyptian Journal of Petroleum (2015). https://doi.org/10.1016/j.ejpe.2015.02.001
[32] Taylor ODS, Cunningham AL, Walshire LA. Development of a near-surface SWRC device (NSD) for measuring suction under low stress environments. Geotechnical Testing Journal (2020). https://doi.org/10.1520/GTJ20190419
[33] Fredlund DG, Rahardjo H, Fredlund MD. Unsaturated soil mechanics in engineering practice. Hoboken, New Jersey: John Wiley & Sons, Inc; (2012). https://doi.org/10.1002/9781118280492
[34] Oh WT, Vanapalli S. Undrained Shear Strength of Unsaturated Soils under Zero or Low Confining Pressures in the Vadose Zone. Vadose Zone Journal (2018). https://doi.org/10.2136/vzj2018.01.0024
[35] Velea D, Shields FD, Sabatier JM. Elastic Wave Velocities in Partially Saturated Ottawa Sand. Soil Science Society of America Journal (2000). https://doi.org/10.2136/sssaj2000.6441226x
[36] Taylor ODS, Cunningham AL, Walker RE, McKenna MH, Martin KE, Kinnebrew PG. The behaviour of near-surface soils through ultrasonic near-surface inundation testing. Near Surface Geophysics (2019). https://doi.org/10.1002/nsg.12045
[37] Umu SU, Onur MI, Okur V, Tuncan M, Tuncan A. Reliability Evaluation of Dynamic Characteristics of Clean Sand Soils Based on Soft Computing Methods. Arab J Sci Eng (2016). https://doi.org/10.1007/s13369-015-1883-7
[38] Kumar Thota S, Duc Cao T, Vahedifard F. Poisson's Ratio Characteristic Curve of Unsaturated Soils. Journal of Geotechnical and Geoenvironmental Engineering (2021). https://doi.org/10.1061/(ASCE)GT.1943-5606.0002424
[39] Suwal LP, Kuwano R. Disk shaped piezo-ceramic transducer for P and S wave measurement in a laboratory soil specimen. Soils and Foundations (2013). https://doi.org/10.1016/j.sandf.2013.06.004
[40] Irfan M, Uchimura T. Modified triaxial apparatus for determination of elastic wave velocities during infiltration tests on unsaturated soils. KSCE Journal of Civil Engineering (2016). https://doi.org/10.1007/s12205-015-0404-2
[41] Mancuso C, Vinale F. Propagazione delle onde sismiche: teoria e misura in sito. Atti del Convegno del Gruppo Nazionale di Coordinamento per gli Studi di Ingegneria Geotecnica, Monselice, Italy. pp. 115–138 [In Italian] (1988)
[42] Fredlund DG, Xing A. Equations for the soil-water characteristic curve. Canadian Geotechnical Journal (1994). https://doi.org/10.1139/t94-061
[43] Linneman DC, Strickland CE, Mangel AR. Compressional wave velocity and effective stress in unsaturated soil: Potential application for monitoring moisture conditions in vadose zone sediments. Vadose Zone Journal (2021). https://doi.org/10.1002/vzj2.20143
[44] Qureshi MU, Towhata I, Yamada S, Aziz M, Aoyama S. Geotechnical risk assessment of highly weathered slopes using seismic refraction technique. In: Prediction and Simulation Methods for Geohazard Mitigation (2009). https://doi.org/10.1201/NOE0415804820
[45] Salem HS. Poisson's ratio and the porosity of surface soils and shallow sediments, determined from seismic compressional and shear wave velocities. Geotechnique (2000). https://doi.org/10.1680/geot.2000.50.4.461
[46] Inci G, Yesiller N, Kagawa T. Experimental Investigation of Dynamic Response of Compacted Clayey Soils. Geotechnical Testing Journal (2003). https://doi.org/10.1520/GTJ11328J